# Equilibrium $\beta$-limits in classical stellarators

**J. LOIZU** [1] †, **S. R. HUDSON** [2], **C. NÜHRENBERG** [1], **AND J. GEIGER** [1]

[1]Max-Planck-Institut für Plasmaphysik, D-17491 Greifswald, Germany

[2]Princeton Plasma Physics Laboratory, PO Box 451, Princeton, New Jersey 08543, USA

(Received 30 April 2017)

A numerical investigation is carried out to understand the equilibrium $\beta$-limit in a classical stellarator. The SPEC code is used in order to assess whether or not magnetic islands and stochastic field-lines can emerge at high $\beta$. Two modes of operation are considered: a *net-current-free stellarator* and a *flux-conserving stellarator*. Despite the fact that relaxation is allowed, the former is shown to maintain good flux surfaces up to the $\beta$-limit predicted by ideal-MHD, above which a separatrix forms. The latter, which has no ideal equilibrium $\beta$-limit, is shown to develop regions of magnetic islands and chaos at sufficiently high $\beta$, thereby providing a "non-ideal $\beta$-limit". Perhaps surprisingly, however, the value of $\beta$ at which the Shafranov shift of the axis reaches a fraction of the minor radius follows *in all cases* the scaling laws predicted by ideal-MHD. We compare our results to the High-Beta-Stellarator theory of (Freidberg 2014).

## 1. Introduction

In stellarators, the maximum achievable $\beta$ is most probably set by the equilibrium and not by its stability (Helander *et al.* 2012). In fact, magnetic surfaces are not guaranteed to exist in three-dimensional MHD equilibria without a continuous symmetry. The potential destruction of magnetic surfaces at sufficiently high $\beta$ can thus lead to the loss of confinement.

The equilibrium $\beta$-limit is not fully understood since it requires the accurate computation of three-dimensional MHD equilibria, which generally consist of an intricate combination of magnetic surfaces, magnetic islands, and magnetic field-line chaos. The Stepped-Pressure Equilibrium Code (SPEC) was developed as one possible approach to fulfil this highly non-trivial task (Hudson *et al.* 2012). SPEC has been rigorously verified in axisymmetry (Hudson *et al.* 2012), in slighlty perturbed configurations (Loizu *et al.* 2015*b*,*a*, 2016*a*), and more recently in stellarator geometries (Loizu *et al.* 2016*b*).

With a view to progressing towards an understanding of the $\beta$-limit in advanced, fusion-relevant stellarator experiments, we focus on a classical stellarator geometry with a simple pressure pedestal and perform a basic numerical study of its equilibrium $\beta$-limit. The simplified geometry allows us to use the High-Beta-Stellarator model (Freidberg 2014) to guide our investigation.

## 2. Model and control parameters

We consider the fixed-boundary problem of a finite $\beta$ equilibrium in a classical $l = 2$ stellarator. Namely, we must provide (i) the geometry of the boundary, e.g. via the Fourier coefficients of the cylindrical coordinates defining the boundary surface, $\{R_{mn}, Z_{mn}\}$; (ii)

† Email address for correspondence: joaquim.loizu@ipp.mpg.de

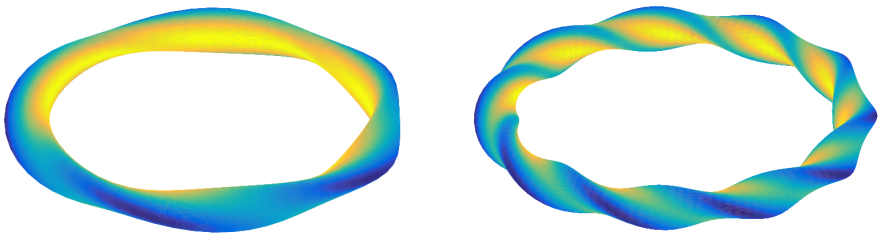

FIGURE 1. Boundary of a classical $l = 2$ stellarator with $N_p = 5$ (left) and $N_p = 10$ (right) field periods. The inverse aspect ratio is $\epsilon = 0.1$ and the colour represents the amplitude of the vacuum magnetic field on the boundary as computed from SPEC.

the pressure profile as a function of the enclosed toroidal magnetic flux, $p(\Psi)$; and (ii) an additional profile, e.g. the rotational transform, $\iota(\Psi)$, or the net toroidal current, $I_\varphi(\Psi)$.

2.0.1. *Boundary*

The simplest boundary representation that can model an $l = 2$ stellarator is that of a rotating ellipse with no toroidally averaged elongation. Namely,

$$\begin{aligned} R(\theta,\varphi) &= R_{00} + R_{10}\cos\theta + R_{11}\cos\left(\theta - N_p\varphi\right) \\ Z(\theta,\varphi) &= Z_{00} + Z_{10}\sin\theta + Z_{11}\sin\left(\theta - N_p\varphi\right) \end{aligned} \tag{2.1}$$

with $Z_{00} = 0$, $Z_{10} = -R_{10}$, and $Z_{11} = R_{11}$. For our $\beta$-limit study, the main parameters of interest in Eq. 2.1 are the major radius, $R_{00}$, and the number of field periods, $N_p$. In fact these can be used to vary independently the inverse aspect ratio, $\epsilon$, and the vacuum rotational transform, $\iota_v$, which are predicted to determine the ideal $\beta$-limit. We therefore choose to fix the other parameters to $R_{10} = 1$ and $R_{11} = 0.25$. Two examples of boundaries with different values of $N_p$ are shown in Fig. 1.

The inverse aspect ratio is

$$\epsilon = \frac{r_{\text{eff}}}{R_{00}} \ , \tag{2.2}$$

where the effective minor radius is $r_{\text{eff}} = \sqrt{r_{\max} r_{\min}}$, with $r_{\max} = R_{10} + R_{11} = 1.25$ and $r_{\min} = R_{10} - R_{11} = 0.75$, respectively the major and minor axis of the rotating ellipse. The vacuum rotational transform can be determined analytically (Helander 2014) as

$$\iota_v = \frac{N_p}{2}\frac{(r_{\max} - r_{\min})^2}{r_{\max}^2 + r_{\min}^2} \ . \tag{2.3}$$

2.0.2. *Pressure profile*

We model a pressure pedestal by assuming that all the pressure gradient is concentrated on a single flux-surface, namely $p(\Psi) = p_0$ for $\Psi \leqslant \Psi_a$ and $p(\Psi) = 0$ for $\Psi \geqslant \Psi_a$. This step in the pressure is naturally described by the SPEC code: two Taylor-relaxed volumes

separated by an ideal-interface supporting a pressure step $[[p]] = p(\Psi_a^+) - p(\Psi_a^-) = p_0$, in correspondence to which a jump in $B$ must arise according to $[[p + \frac{B^2}{2\mu_0}]] = 0$. This implies the presence of a surface current that is simply a weak representation of the pressure-driven (diamagnetic and Pfirsch-Schlüter) current. For our basic $\beta$-limit study, we choose to fix the value $\Psi_a = 0.3\Psi_{\rm edge}$ and use the freedom in $p_0$ to control the value of $\beta$, which we define here as $\beta = 2\mu_0 p_0/B_0^2$, where $B_0 = B(\Psi = 0)$.

2.0.3. *Net-current-free versus flux-conserving*

The SPEC code calculates MHD equilibria as extrema of the Multiregion, Relaxed MHD (MRxMHD) energy functional (Hole *et al.* 2007; Hudson *et al.* 2007). In essence, the energy functional is the same as in conventional ideal MHD equilibrium theory, but the constraints under which the function is extremized are different. While in ideal-MHD the magnetic topology is *continuously* constrained, in MRxMHD the topology is only *discretely* constrained, thus allowing for partial relaxation. More precisely, the plasma is partitioned into a finite number, $N_V$, of nested volumes, $V_v$, that undergo Taylor relaxation. These volumes are separated by $N_V - 1$ interfaces that are constrained to remain magnetic surfaces during the energy minimization process. For the $\beta$-limit study at hand, we have $N_V = 2$ volumes separated by one ideal-interface. The location and shape of this interface is unkown *a priori* and determined self-consistently by a force-balance condition. MRxMHD equilibrium states satisfy

$$\nabla \times \mathbf{B} = \mu_v \mathbf{B} \quad \text{in the volumes} \tag{2.4}$$

$$\left[\left[p + \frac{B^2}{2\mu_0}\right]\right] = 0 \quad \text{on the interface} \tag{2.5}$$

for $v = 1, 2$. In addition to providing the enclosed toroidal fluxes in each volume ($\Psi_a$ and $\Psi_{\rm edge}$), the solution to Eq. 2.4 requires one more parameter if the volume is a topological torus (the innermost volume) and two more parameters if the volume is an annulus (the outer volume). Hence we must provide a total of 3 parameters to determine the equilbrium solution at a given value of $\beta$.

If we want to enforce a zero net-toroidal-current, $I_\varphi = 0$, we can impose $\mu_1 = \mu_2 = 0$ and then iterate on the total enclosed poloidal flux, $\psi_p$, until the surface current has no net toroidal component. At each iteration step, the net toroidal surface current can be easily calculated as

$$I_\varphi^{\rm CS} = \int_0^{2\pi} [[\mathbf{B}]] \cdot \mathbf{e}_\theta \; d\theta \tag{2.6}$$

by virtue of Ampere's law. The iterative procedure can be implemented via a Newton method and brings $I_\varphi^{CS}$ down to machine precision in a few steps. We refer to this mode of operation as *zero-net-current*.

If we want to constrain the rotational transform, $\iota(\Psi)$, we can enforce it to remain constant on both sides of the ideal-interface, $\iota_a^+ = \iota_a^- = \iota_a$, and at the edge, $\iota_{\rm edge}$. Once again, this can be achieved by iterating on the values of $\mu_{1,2}$ and $\psi_p$. We refer to this mode of operation as *flux-conserving*.

We would like to remark that while the *zero-net-current* mode guarantees $I_\varphi = 0$, it does not guarantee that the rotational transform remains constant, and in particular we expect $\iota_a^+ \neq \iota_a^-$. Conversely, the *flux-conserving* mode guarantees that $\iota$ remains constant on certain surfaces (thus only locally flux-conserving) but in general we expect $I_\varphi \neq 0$, in particular at the location of the pressure-gradient.

## 3. High-$\beta$ equilibria and Shafranov shift

Figure 2 shows Poincaré plots of the equilibirium magnetic field at different values of $\beta$ for both the *zero-net-current* stellarator and the *flux-conserving* stellarator. In both cases there is a Shafranov shift that increases with $\beta$. However, the Shafranov shift of the axis, $\Delta_{\rm ax}$, increases with $\beta$ much faster in the *zero-net-current* stellarator. It is useful to define the quantity

$$\beta_{0.5} \equiv \beta(\Delta_{\rm ax} = \frac{r_{\rm eff}}{2}) \ , \tag{3.1}$$

namely, the value of $\beta$ at which the Shafranov shift of the axis reaches half of the minor radius. According to ideal-MHD equilbrium theory (Miyamoto 2005), $\beta_{0.5}$ is predicted to scale as

$$\beta_{0.5} \sim \epsilon \ \iota_v^2 \sim \frac{N_p^2}{R_{00}} \tag{3.2}$$

for large aspect ratios, $\epsilon \ll 1$, and slowly varying $\iota_v$, which is true for $\iota_v \ll 1$. A scan in both $R_{00}$ and $N_p$ has been carried out in order to assess how $\beta_{0.5}$ scales in the numerical MHD calculations. Figure 3 shows the result of this scan. Despite the fact that SPEC allows for plasma relaxation, the scaling law 3.2 is very well reproduced in both modes of operation. However, the values of $\beta_{0.5}$ are much higher in the *flux-conserving* stellarator, by a factor of about 6. This can be explained in terms of the High-Beta-Stellarator (HBS) model developed in (Freidberg 2014).

## 4. $\beta$-limits and the HBS theory

The HBS model for a classical stellarator developed in (Freidberg 2014) predicts that the rotational transform at the plasma edge, $\iota_a$, evolves with $\beta$ and plasma current as

$$\iota_a = (\iota_v + \iota_I) \left(1 - \nu^2\right)^{1/2} \tag{4.1}$$

where $\iota_I$ is the transform produced by the net toroidal current,

$$\iota_I = \frac{\mu_0 I_\varphi}{2\pi a^2 B_0} \ , \tag{4.2}$$

and

$$\nu = \frac{\beta}{\epsilon_a (\iota_v + \iota_I)^2} \ , \tag{4.3}$$

where $a$ is the effective minor radius of the plasma edge and $\epsilon_a = a/R$. For our system, we have $a = \sqrt{\Psi_a/\Psi_{\rm edge}} r_{\rm eff}$ and thus $\epsilon_a = \sqrt{\Psi_a/\Psi_{\rm edge}}\epsilon$. In the context of the HBS theory, the *zero-net-current* stellarator can be analyzed by taking $\iota_I = 0$. Equation 4.1 then implies that $\iota_a$ decreases with increasing $\beta$. This is visible in Figure 4, where the profile $\iota(\Psi)$ is shown for a given *zero-net-current* stellarator SPEC equilibrium at finite $\beta$. A jump in the rotational transform self-consistently develops on the ideal interface supporting the pressure gradient, namely at $\Psi_a = 0.3\Psi_{\rm edge}$. The ideal MHD equilibirum code VMEC was also run for this case and shown to produce essentially the same transform profile (in VMEC the pressure pedestal has a finite width). In Fig. 5, the value of $\iota_a$ is shown as a function of $\beta$ and compared to the HBS prediction, Eq. 4.1, showing excellent agreement. The point where $\iota_a = 0$ corresponds to the emergence of a separatrix (see, e.g., Fig. 2) and this defines the ideal $\beta$-limit, namely

$$\beta_{lim} = \epsilon_a \iota_v^2 \ . \tag{4.4}$$

For the *flux-conserving* stellarator, we can impose $\iota_a = \iota_v$ in the HBS model. This leads

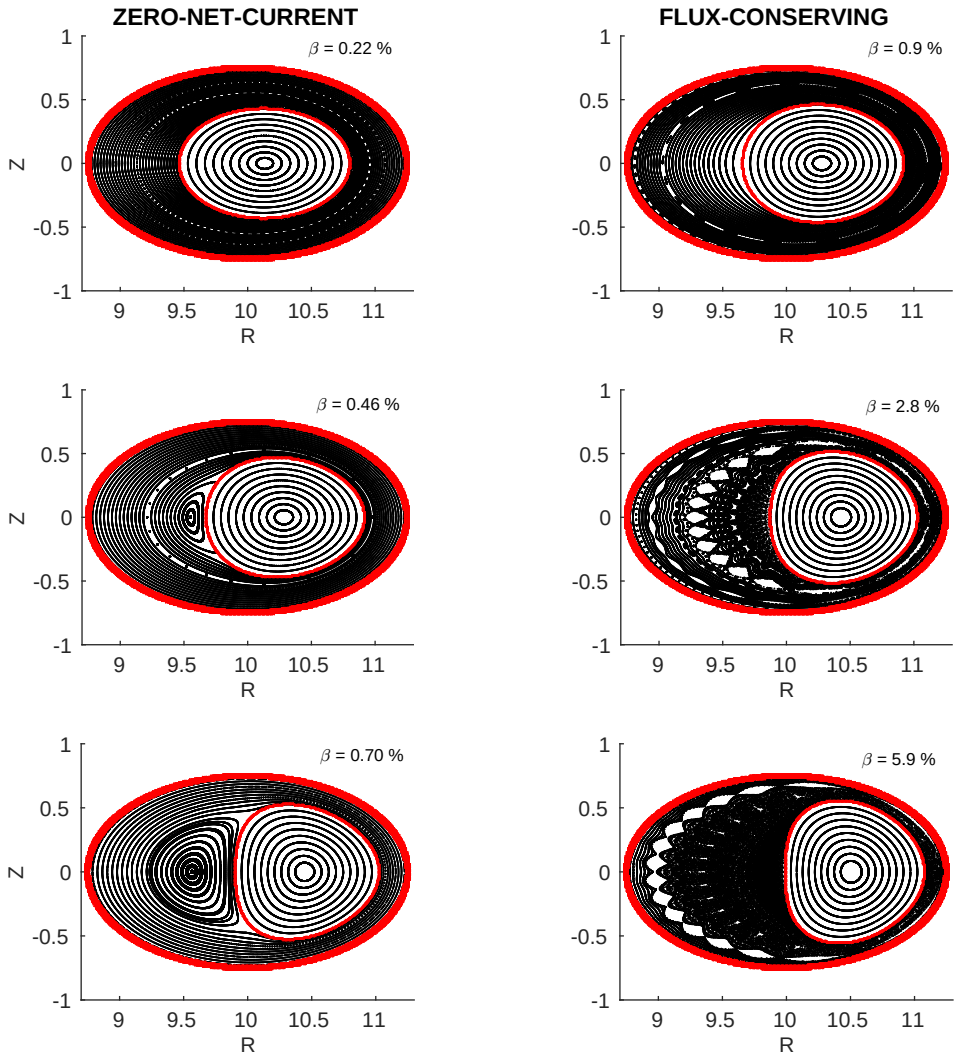


FIGURE 2. Poincaré section ($\varphi = 0^\circ$) of the equilibrium magnetic field at different values of $\beta$. Left: *zero-net-current* stellarator. Right: *flux-conserving* stellarator. Here $N_p = 5$ and $\epsilon = 0.1$.

to an expression for the value of the plasma current that is necessary to maintain $\iota_a$ constant. One obtains (Freidberg 2014)

$$\iota_I = \iota_v \left( \sqrt{\frac{1}{2}\left(1 + \sqrt{1 + 4H^2}\right)} - 1 \right) , \tag{4.5}$$

where

$$H = \frac{\beta}{\epsilon_a \iota_v^2} . \tag{4.6}$$

Figure 6 shows the net toroidal surface current in SPEC equilibria as a function of $\beta$ and compares it to the HBS prediction, Eq. 4.5, showing very good agreement. For large $H \gg 1$, one has $I_\varphi \sim \sqrt{\beta}$, and the HBS model predicts that no $\beta$-limit is reached because

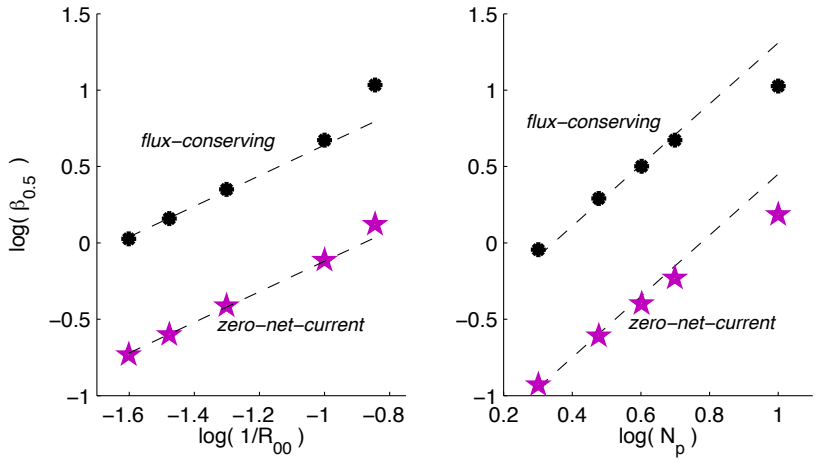


FIGURE 3. Scaling of $\beta_{0.5}$ with the inverse aspect ratio, $\epsilon \sim 1/R_{00}$ (left), and with the vacuum iota, $\iota_v \sim N_p$ (right). Black stars are for the *flux-conserving* stellarator. Magenta pentagrams are for the *zero-net-current* stellarator. The dashed lines have slope 1 (left) and 2 (right).

the plasma current keeps rising and preventing the separatrix to form. From SPEC equilibrium calculations, however, where plasma relaxation is allowed, we observe that magnetic islands and chaotic field-lines emerge at sufficiently high $\beta$, thereby providing a "non-ideal $\beta$-limit". In all the *flux-conserving* stellarator calculations, the emergence of chaos seems to happen always at values of $\beta$ at which the Shafranov shift is about half the minor radius, i.e. $\beta_{lim} \approx \beta_{0.5}$. The exact mechanism explaining this transition is under investigation. We can nevertheless quantify the emergence of chaos by calculating the fractal dimension of the field-lines on the Poincare section as a function of $\beta$ (Meiss 1992). More precisely, we can evaluate the so-called *box-counting* dimension, or *Hausdorff* dimension,

$$D = \lim_{L \to 0} \frac{\log(N)}{\log(L)} \tag{4.7}$$

where $L$ is the size of the boxes and $N$ is the number of boxes containing at least one point of the magnetic field-line on the Poincaré section. If the field-line traces a magnetic surface, or even a magnetic island, one expects $D = 1$. If the magnetic field-line trajectory is chaotic, however, it fills up a certain "area" in the Poincaré section, and $D > 1$ is expected. We calculated the value of $D$ for a given *flux-conserving* stellarator and found that field-lines abruptly transition from $D = 1$ (at low $\beta$) to $D = 1.7$ (at sufficiently high $\beta$), such that the fraction of the of field-lines with $D = 1.7$ smoothly increases with $\beta$.

The authors would like to thank Per Helander, Sam Lazerson, and Jörgen Nührenberg for useful discussions. This work has been carried out in the framework of the EUROfusion Consortium and has received funding from the Euratom research and training programme 2014-2018 under Grant Agreement No. 633053. The views and opinions expressed herein do not necessarily reflect those of the European Commission.

## REFERENCES

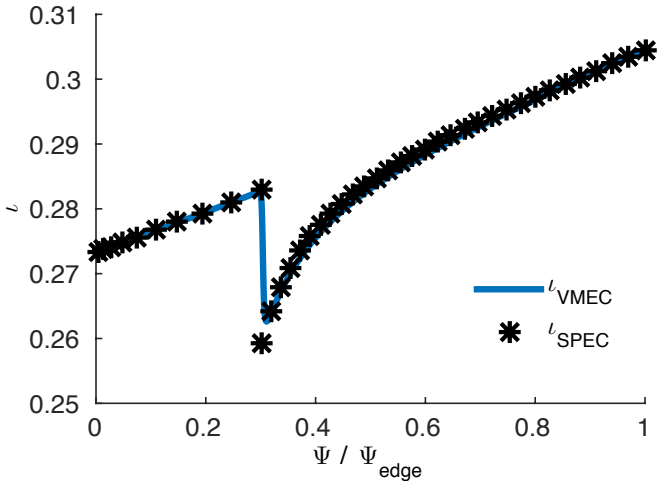


FIGURE 4. Rotational transform as a function of toroidal magnetic flux from both SPEC (black stars) and VMEC (solid blue line). Here $N_p = 5$, $\epsilon = 0.1$, and $\beta = 0.15\%$.

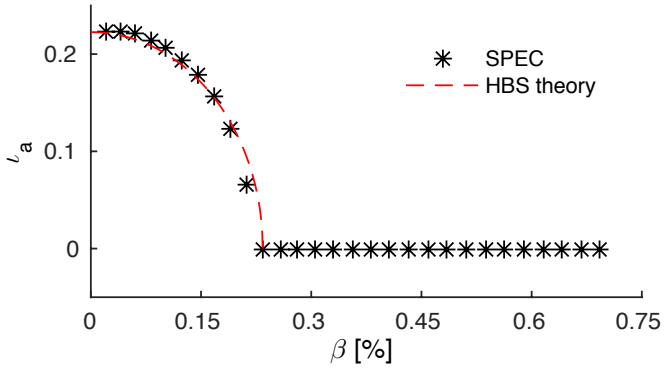


FIGURE 5. Rotational transform at the plasma edge as a function of $\beta$, from SPEC (black stars) and from Eq. 4.1 (dashed red line). Here $N_p = 4$ and $\epsilon = 0.1$.

FREIDBERG, J P 2014 *ideal MHD*. Cambridge University Press.

HELANDER, P. 2014 Theory of plasma confinement in non-axisymmetric magnetic fields. *Reports on Progress in Physics* **77** (8), 087001.

HELANDER, P, BEIDLER, C D, BIRD, T M, DREVLAK, M, FENG, Y, HATZKY, R, JENKO, F, KLEIBER, R, PROLL, J H E, TURKIN, YU & XANTHOPOULOS, P 2012 Stellarator and tokamak plasmas: a comparison. *Plasma Physics and Controlled Fusion* **54** (12), 124009.

HOLE, M.J, HUDSON, S.R & DEWAR, R.L 2007 Equilibria and stability in partially relaxed plasmavacuum systems. *Nuclear Fusion* **47** (8), 746–753.

HUDSON, S. R., DEWAR, R. L., DENNIS, G., HOLE, M. J., MCGANN, M., VON NESSI, G. & LAZERSON, S. 2012 Computation of multi-region relaxed magnetohydrodynamic equilibria. *Physics of Plasmas* **19** (11).

HUDSON, S. R., HOLE, M. J. & DEWAR, R. L. 2007 Eigenvalue problems for Beltrami fields arising in a three-dimensional toroidal magnetohydrodynamic equilibrium problem. *Physics of Plasmas* **14** (5).

LOIZU, J., HUDSON, S., BHATTACHARJEE, A. & HELANDER, P. 2015*a* Magnetic islands and sin-

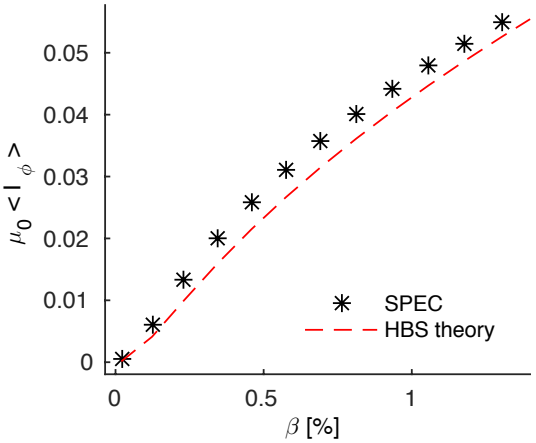


FIGURE 6. Net toroidal plasma current as a function of $\beta$, from SPEC calculations (black stars) and from Eq. 4.5 (dashed red line). Here $N_p = 5$ and $\epsilon = 0.1$.

gular currents at rational surfaces in three-dimensional magnetohydrodynamic equilibria. *Physics of Plasmas* **22** (2).

LOIZU, J., HUDSON, S. R., BHATTACHARJEE, A., LAZERSON, S. & HELANDER, P. 2015*b* Existence of three-dimensional ideal-magnetohydrodynamic equilibria with current sheets. *Physics of Plasmas* **22** (9), 090704.

LOIZU, J., HUDSON, S. R., HELANDER, P., LAZERSON, S. A. & BHATTACHARJEE, A. 2016*a* Pressure-driven amplification and penetration of resonant magnetic perturbations. *Physics of Plasmas* **23** (5).

LOIZU, J., HUDSON, S. R. & N??HRENBERG, C. 2016*b* Verification of the SPEC code in stellarator geometries. *Physics of Plasmas* **23** (11).

MEISS, J. D. 1992 Symplectic maps, variational principles, and transport. *Reviews of Modern Physics* **64** (3), 795–848.

MIYAMOTO, K 2005 *Plasma Physics and Controlled Nuclear Fusion*. Berlin: Springer-Verlag.